

1 **MUMBA Overview - response to reviewers**

2 (1) Comments from Referees

3 **Anonymous Referee #1**

4 **Received and published: 20 March 2017**

5 I read this manuscript with fascination, and have no worry about the publication. The  
6 authors, and collaborators, have developed an innovative monitoring campaign. It is  
7 obvious that the paper was prepared by authors experienced in writing this type of  
8 article.

9 The manuscript describes the MUMBA campaign (e.g. context, background, technological  
10 design) designed to characterize atmospheric composition in a complex environment.

11 This manuscript reports novel approaches and the research direction. The  
12 datasets provide i) a useful case study for validation of coupled models (air quality and  
13 meteorology) in a coastal environment and ii) a basis for scientific papers (in preparation).  
14

15 **Anonymous Referee #2**

16 **Received and published: 4 April 2017**

17 The manuscript submitted by Paton-Walsh et al. describes a dataset for MUMBA campaign,  
18 which took place in a small coastal city in Australia, with the goal to provide information on  
19 atmospheric composition changes under the influences of marine air or urban and biogenic  
20 emissions. The dataset contains time series related to particles, atmospheric trace gases,  
21 speciated VOCs, radon and meteorological parameters. What makes it most interesting is that  
22 campaign captured two extreme heat events and a period when the site was under the  
23 influence of clean marine air. The provided dataset can be used for testing the chemical  
24 transport models, but not only. Present paper also introduces the future ones focused on  
25 specific issues mentioned in the Summary and Conclusion section.

26 The manuscript is logically structured and provides a good overview of the available  
27 information gathered during the measurement campaign. It is a well-written data description  
28 paper. Abstract is a good representation of the main text, the instrumentation  
29 is presented in necessary detail, the experimental methods are currently used in the  
30 field, enough explained and with references when it was necessary. The accuracy of  
31 the resulting dataset appears to be adequate. The data files are indeed public, easily  
32 accessible (under Creative Commons Attribution License) in many formats and the  
33 Summary and Conclusion section of the manuscript mentions clearly that MUMBA data  
34 is free to the scientific community.  
35

36 I recommend publication of this work, subject to the very few minor comments:  
37

- 38 1.) The authors should give more details on pollution sources in the metropolitan area in  
39 Section 2.

1 2.) The authors state their MUMBA campaign period runs from 21st December 2012 to  
2 15th February 2013. However, the dataset on PM<sub>2.5</sub> indicates data from 24-25 January  
3 to 15 February; carbonyls - only in February 2013; CN/CCN – from 16/15 January to 15  
4 February; carbon fractions – from 22 January to 15 February... Although the authors  
5 indicate this in Table 1 and make a short statement in Section 3, it is not easy for  
6 reader to get a clear image of the different periods associated to the various measured  
7 parameter. I think a more elaborate explanation of these discrepancies should be  
8 added in Section 3. There are some negative values in the data set that should be also  
9 explained.

10 3.) Page 6, line 21: please, replace "all times are reported in: : :" with "all measurements  
11 are reported in: : :"

12 4.) Page 11, line 4 and line 15: please, replace "diel cycles" with "diurnal cycles".  
13

## 14 **(2) Author's response and (3) Author's changes to manuscript.**

15 The authors would like to thank the reviewers for their time and positive comments on the  
16 manuscript.

17 The specific points raised by reviewer 2 are addressed below:

18 1.) Agreed – the following sentence has been added at page 4, line 19: “*The steelworks  
19 and surrounding industry is a large source of PM<sub>2.5</sub> and CO, whilst traffic dominates  
20 the remainder of the urban pollution sources.*”

21 2.) Agreed.

22 a) Campaign periods: We tried to make this clear in Table 1 but have tried to further  
23 clarify this in the main text (page 6, line 12), which now reads: ” *All  
24 measurements made during the campaign are listed in Table 1, along with the  
25 dates of operation for each instrument. MUMBA operated in two distinct stages,  
26 with most gas-phase and meteorological measurements running throughout the 8  
27 week campaign, and aerosol-phase measurements added in the second half of the  
28 campaign. A few instruments operated for different time periods and these are  
29 distinguished in Table 1 by different background shading.*”

30 b) Negative values: The following sentences were added: “*Note that some  
31 instruments can produce negative values when the concentrations are close to the  
32 detection limit. Negative concentration values (although non-physical) have not  
33 been removed from the MUMBA dataset because they are indicative of the  
34 instruments’ true performance and removing negative values will produce small  
35 positive biases in calculations of longer term average concentrations.*”:

36  
37 3.) Agreed - Done

38 4.) Agreed - Done  
39  
40

41 The corrected manuscript is shown below:

1           **THE MUMBA CAMPAIGN: MEASUREMENTS OF**  
2           **URBAN, MARINE AND BIOGENIC AIR**

3  
4           **Clare Paton-Walsh<sup>1\*</sup>, Élise-Andrée Guérette<sup>1</sup>, Dagmar Kubistin<sup>1</sup>, Ruhi Humphries<sup>1,2</sup>,**  
5           **Stephen R. Wilson<sup>1</sup>, Doreena Dominick<sup>1</sup>, Ian Galbally<sup>1,2</sup>, Rebecca Buchholz<sup>1,3</sup>,**  
6           **Mahendra Bhujel<sup>1,2</sup>, Scott Chambers<sup>4</sup>, Min Cheng<sup>2</sup>, Martin Cope<sup>2</sup>, Perry Davy<sup>5</sup>,**  
7           **Kathryn Emmerson<sup>2</sup>, David W. T. Griffith<sup>1</sup>, Alan Griffiths<sup>4</sup>, Melita Keywood<sup>2</sup>,**  
8           **Sarah Lawson<sup>2</sup>, Suzie Molloy<sup>2</sup>, Géraldine Rea<sup>1,6</sup>, Paul Selleck<sup>2</sup>, Xue Shi<sup>1</sup>, Jack**  
9           **Simmons<sup>1</sup> and Voltaire Velazco<sup>1</sup>**

10  
11           <sup>1</sup> Centre for Atmospheric Chemistry, School of Chemistry, University of Wollongong,  
12           Northfields Avenue, Wollongong, N.S.W. Australia.

13           <sup>2</sup> CSIRO Climate Science Centre, Aspendale, Victoria, Australia.

14           <sup>3</sup> Atmospheric Chemistry Observations & Modeling (ACOM) Laboratory, National Center for  
15           Atmospheric Research, Boulder, CO, USA

16           <sup>4</sup> ANSTO, Environmental Research, Locked Bag 2001, Kirrawee DC, NSW 2232, Australia.

17           <sup>5</sup> GNS Science, National Isotope Centre, Lower Hutt, NZ.

18           <sup>6</sup> Université Pierre et Marie Curie, Laboratoire de Météorologie Dynamique - CNRS/IPSL  
19           Ecole Polytechnique 91128 Palaiseau Cedex, Paris, France.

20  
21           \* Author to whom correspondence should be addressed; Clare Paton-Walsh (Murphy)  
22           (E-Mail: [clarem@uow.edu.au](mailto:clarem@uow.edu.au)); Tel.: +61-2-4221-5065; Fax: +61-2-4221-4287;

## 1 **Abstract**

2 The Measurements of Urban, Marine and Biogenic Air (MUMBA) campaign took place in  
3 Wollongong, New South Wales (a small coastal city approximately 80 km south of Sydney,  
4 Australia), from 21<sup>st</sup> December 2012 to 15<sup>th</sup> February 2013. Like many Australian cities,  
5 Wollongong is surrounded by dense eucalyptus forest and so the urban air-shed is heavily  
6 influenced by biogenic emissions. Instruments were deployed during MUMBA to measure  
7 the gaseous and aerosol composition of the atmosphere with the aim of providing a detailed  
8 characterisation of the complex environment of the ocean/forest/urban interface that could be  
9 used to test the skill of atmospheric models. Gases measured included ozone, oxides of  
10 nitrogen, carbon monoxide, carbon dioxide, methane and many of the most abundant volatile  
11 organic compounds. Aerosol characterisation included total particle counts above 3 nm, total  
12 cloud condensation nuclei counts; mass concentration, number concentration size  
13 distribution, aerosol chemical analyses and elemental analysis.

14 The campaign captured varied meteorological conditions, including two extreme heat events,  
15 providing a potentially valuable test for models of future air quality in a warmer climate.  
16 There was also an episode when the site sampled clean marine air for many hours, providing  
17 a useful additional measure of background concentrations of these trace gases within this  
18 poorly sampled region of the globe. In this paper we describe the campaign, the meteorology  
19 and the resulting observations of atmospheric composition in general terms, in order to equip  
20 the reader with sufficient understanding of the Wollongong regional influences to use the  
21 MUMBA datasets as a case study for testing a chemical transport model. The data is  
22 available from PANGAEA (see <http://doi.pangaea.de/10.1594/PANGAEA.871982>).

23

24

25 **Keywords:** VOCs, Ozone, Greenhouse Gases, Aerosols, Air Quality, Measurement  
26 Campaign,

27

## 28 **1. Introduction**

29 The value of intensive measurement campaigns in helping to understand and characterise  
30 local atmospheric composition and air quality has been recognised from as early as 1969,  
31 when the Los Angeles Smog Project took place [*Whitby et al.*, 1972b]. Since then, many such  
32 campaigns have focused on understanding the formation of photochemical smog in the most  
33 polluted cities worldwide, with early efforts concentrated in the USA, (e.g. in [*Gray et al.*,  
34 1986; *Husar et al.*, 1972; *Whitby et al.*, 1972a]). The formation of secondary organic aerosol  
35 has also been of particular interest, with many studies using elemental carbon (black carbon)  
36 as an indicator of primary emissions; when the ratio of organic carbon to elemental carbon in  
37 the sampled air is higher than expected from the ratio of the primary emissions, secondary  
38 organic aerosol formation is indicated [*Castro et al.*, 1999; *Gray et al.*, 1986; *Turpin and*  
39 *Huntzicker*, 1995].

1 In Australia, there have been a number of studies aimed at improving our understanding of  
2 ozone chemistry in the cleaner southern hemisphere atmosphere [Galbally *et al.*, 2000;  
3 Monks *et al.*, 1998]; secondary aerosol formation [Caine *et al.*, 2007] or other air quality  
4 issues, such as air toxics and smoke [Hinwood *et al.*, 2007; Keywood *et al.*, 2015]. There have  
5 also been some air quality studies specifically aimed at testing the Australian Air Quality  
6 Forecasting System [Cope *et al.*, 2004] in Sydney [Hess *et al.*, 2004] and Melbourne [Tory *et al.*,  
7 2004]. The primary focus of these studies was testing the prediction of ozone levels in the  
8 urban environment [Cope *et al.*, 2005]. More recent studies have examined regional air  
9 quality in Wollongong [Buchholz *et al.*, 2016] and the effect of a major fire event on air  
10 quality in Sydney and Wollongong [Rea *et al.*, 2016]. There have also been Australian  
11 campaigns focused on understanding aerosol formation and composition, in the urban  
12 environment e.g. [Cheung *et al.*, 2011; Cheung *et al.*, 2012]; coastal environments [Caine *et al.*,  
13 2007; Fletcher *et al.*, 2007; Modini *et al.*, 2009] and within eucalypt forests [Ristovski *et al.*,  
14 2010; Suni *et al.*, 2008]. In addition, there have been some detailed studies to characterise  
15 the concentrations of VOCs in the clean background atmosphere in the Australasian region  
16 [Colomb *et al.*, 2009; Galbally *et al.*, 2007; Lawson *et al.*, 2015].

17 In this overview paper, we describe a measurement campaign in the small Australian coastal  
18 city of Wollongong, of approximately 292,000 residents. The Wollongong region is bounded  
19 by ocean to the east and by a steep escarpment, covered in eucalypt forest, to the west. The  
20 coastal plain is roughly triangular in shape, being very narrow in the north where the  
21 escarpment meets the sea, and roughly 20 kilometres wide in the south. The region spans  
22 about 50 kilometres of coastline.

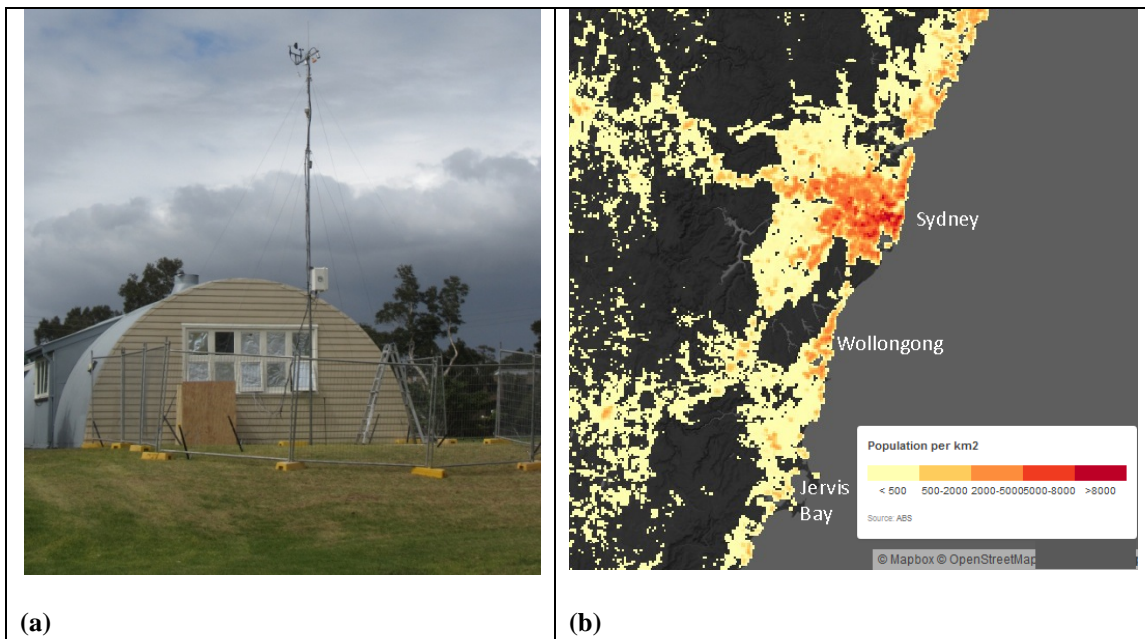
23 The MUMBA campaign involved collaboration between three Australian research groups  
24 (the University of Wollongong; the Commonwealth Scientific and Industrial Research  
25 Organisation (CSIRO), and the Australian Nuclear Science and Technology Organisation  
26 (ANSTO), and one research organisation from New Zealand (GNS Science). MUMBA was  
27 designed to provide a comprehensive characterisation of the local atmosphere that could test  
28 the capabilities of air quality models to forecast atmospheric composition. Influences from  
29 the nearby ocean sources, urban emissions and the biogenic emissions from the surrounding  
30 eucalypt forests were expected to impact the site. This campaign aimed to make detailed  
31 measurements of atmospheric composition under the combined influence of these different  
32 sources, all of which typically affect the populated regions of the East coast of Australia.

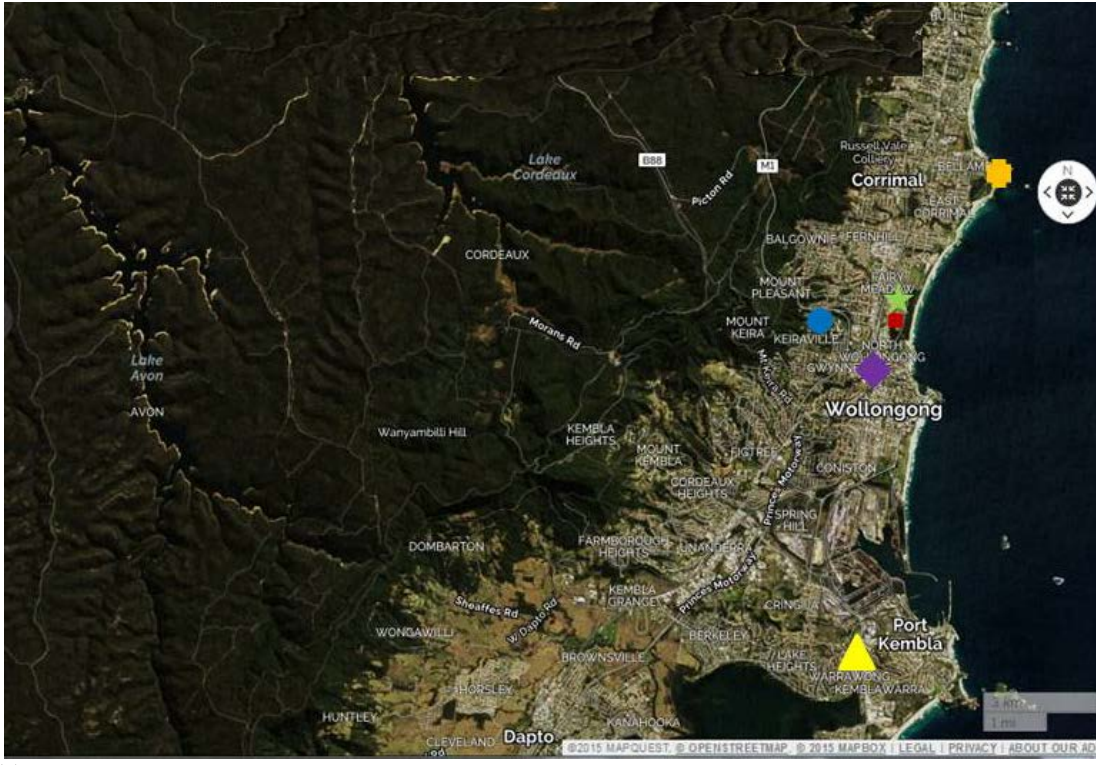
## 33 **2. Measurement Sites**

34 The MUMBA campaign included instruments that were run at several different, nearby sites.  
35 The main measurement site (34.397°S, 150.900°E) of the MUMBA campaign was located in  
36 a suburban area of Wollongong approximately half a kilometre from the ocean. The  
37 instruments were located in and adjacent to an unused hut located at the University of  
38 Wollongong's campus east (see Figure 1a). Most instruments sampled from a mast at a height  
39 of ~10 m above the surrounding ground level (also shown in Figure 1a). Immediately  
40 surrounding the measurement site is a grassy plain with a suburban road to the east and a strip  
41 of forested parkland beyond, before the sand dunes and ocean. Prevailing easterly sea breezes

1 brought air-masses from the ocean to the site during the day. Urban influences from the local  
2 metropolitan area and a large industrial area, including a steelworks, typically occurred in  
3 still conditions or with southerly winds. The steelworks and surrounding industry is a large  
4 source of  $PM_{2.5}$  and CO, whilst traffic dominates the remainder of the urban pollution  
5 sources. The steep forested escarpment is about 3 km directly to the west of the site and  
6 approximately 400 m high, with the area beyond dominated by eucalypt forest, such that  
7 westerly winds brought strong biogenic signals. The population density within the  
8 surrounding area of New South Wales (NSW), including Wollongong and Sydney is shown  
9 in Figure 1b.

10 The locations of different measurement sites are shown in Figure 1c.





(c)

Figure 1: (a) Hut that hosted most of the instruments during MUMBA and the sample mast. (b) Population density map for the region based on Australian Bureau of Statistics data from August 2011 – <http://www.abs.gov.au/AUSSTATS/abs@.nsf/Lookup/1270.0.55.007Main+Features12011?OpenDocument> (c) Satellite view of the region showing the main MUMBA site (green star), the Wollongong Science Centre (red square), Wollongong EPA Air Quality station (purple diamond), the University of Wollongong (blue circle), Bellambi Automatic Weather Station (orange hexagon) and the ANSTO radon detector site at Warrawong (yellow triangle). The large red square indicates the approximate location of the CHIMERE grid-space used to compare to the MUMBA observations. Also visible is the large industrial area at Port Kembla and the extensive forested regions to the West. The image was created using website: [www.mapquest.com](http://www.mapquest.com) “© OpenStreetMap contributors”.

In addition, ANSTO provided measurements of atmospheric radon concentrations from Warrawong (34.48°S, 150.89°E), an industrial suburban site located approximately 10 km to the south of the main MUMBA site. The use of radon to characterise boundary layer mixing [Chambers *et al.*, 2011] is likely to be especially useful for testing air quality models, due to the challenges of modelling within the complex topography of coastal areas. The locations of all of the sites used in the MUMBA campaign are marked on the satellite view of the region shown in Figure 1c.

### 3. Description of the Instruments Deployed at the Main Measurement Site

A large range of instrumentation was deployed to enable a detailed characterisation of atmospheric composition during the campaign. All measurements made during the campaign are listed in Table 1, along with the dates of operation for each instrument. MUMBA

1 operated in two distinct stages, with most gas-phase and meteorological measurements  
2 running throughout the 8 week campaign, and aerosol-phase measurements added in the  
3 second half of the campaign. A few instruments operated for different time periods and these  
4 are distinguished in Table 1 by different background shading. All data are available from  
5 PANGAEA (<https://doi.pangaea.de/10.1594/PANGAEA.871982>) as hourly averages unless  
6 otherwise specified. Further details of the instruments are given in the Appendix, along with a  
7 second table that lists the specific VOCs measured during the campaign and their limits of  
8 detection. Note that some instruments can produce negative values when the concentrations  
9 are close to the detection limit. Negative concentration values (although non-physical) have  
10 not been removed from the MUMBA dataset because they are indicative of the instruments'  
11 true performance and removing negative values will produce small positive biases in  
12 calculations of longer term average concentrations. Also available from PANGAEA are the  
13 radon measurements made at Warrawong by ANSTO and the air quality data from the  
14 Wollongong Office of Environment and Heritage (OEH) station. The FTIR spectrometer  
15 uses a drier on the inlet and measured mole fraction in dry air; other gas phase instruments  
16 measured in ambient air. All measurements are reported in local standard time (UTC +10).

#### 17 **4. Additional Measurements**

18 Measurements were also available from the OEH air quality station at Wollongong  
19 (34.419°S, 150.886°E). Additional instruments were operated nearby at the University of  
20 Wollongong's main campus (at 34.406°S, 150.897°E) [*Buchholz et al.*, 2016] and at the  
21 nearby Science Centre (34.401°S, 150.900°E), but the observations are not included here.  
22 Data from the University of Wollongong include retrievals of total column amounts of trace  
23 gases from the Total Carbon Column Observing Network (see <http://www.tccon.caltech.edu/>)  
24 and the Network for Detection of Atmospheric Composition Change (see  
25 <http://www.ndsc.ncep.noaa.gov/>) and in situ greenhouse gas measurements (see  
26 <http://doi.pangaea.de/10.1594/PANGAEA.848263>). The instrument installed at the Science  
27 Centre was a Multi-Axis Differential Optical Absorption Spectrometer, and the data is  
28 available from the authors upon request. The Australian Bureau of Meteorology operates an  
29 Automatic Weather Station (AWS) at Bellambi (34.37°S, 150.93°E). Again, the data are not  
30 included here but can be requested from the Bureau if needed.

1 **Table 1: Measurements made during the MUMBA campaign, tabulated alongside the time resolution, the instrument type, and the dates the instrument was**  
 2 **operational. Instruments which ran for the full 8 weeks of the MUMBA campaign are shaded in dark grey, aerosol instruments that ran for the second half of the**  
 3 **campaign are shaded in light grey and instruments that ran for a shorter time period have a white background.**

Measured Parameter(s)	Instrument/Technique	Measurement Time Resolution	Reported Time Resolution	Reported units	Measurement Period
O <sub>3</sub>	UV (Thermo 49i)	1 min	1 hr	ppb	Dec 21 <sup>st</sup> – Feb 15 <sup>th</sup>
NO NO <sub>2</sub> +	Chemiluminescence, (Thermo 42i) molybdenum converter	1 min	1 hr	ppb	Dec 21 <sup>st</sup> – Feb 15 <sup>th</sup>
VOCs	PTR-MS (Ionicon)	~3 min	1 hr	ppb	Dec 21 <sup>st</sup> – Feb 15 <sup>th</sup>
CO <sub>2</sub> CO, CH <sub>4</sub> , N <sub>2</sub> O del <sup>13</sup> C in CO <sub>2</sub>	FTIR in situ analyser	~3 min	1 hr	ppm ppb per mille	Dec 21 <sup>st</sup> – Feb 15 <sup>th</sup>
Boundary layer height	Elastic backscatter at 355nm - LIDAR (Leosphere ALS-400)	30 s	20 minutes	metres above ground level	Dec 21 <sup>st</sup> – Feb 15 <sup>th</sup>
wind speed wind direction temperature pressure relative humidity	Campbell Scientific EasyWeather	1 min 5 min	1 hr 1 hr	m/s degrees degree Celsius mbar %	Dec 21 <sup>st</sup> – Jan 25 <sup>th</sup> Jan 25 <sup>th</sup> – Feb 15 <sup>th</sup>
Total number concentration of condensation nuclei >3nm	Ultrafine Condensation Particle Counter (TSI 3776)	1 s	1 hr	particles/cm <sup>3</sup>	Jan 16 <sup>th</sup> – Feb 15 <sup>th</sup>
Total number concentration of cloud condensation nuclei	Cloud Condensation Nuclei Counter (Droplet Measurement Technologies)	1 s	1 hr	particles/cm <sup>3</sup>	Jan 16 <sup>th</sup> – Feb 15 <sup>th</sup>
Particle number size distribution (~14 nm to ~660 nm)	Scanning mobility particle sizer	~ 5 min	1 hr	diameter: nm particle concentration: dN/dLogDp particles/cm <sup>3</sup>	Jan 16 <sup>th</sup> – Feb 15 <sup>th</sup>
Elemental and organic carbon in PM <sub>2.5</sub> fraction	HiVol sampling – chemical analysis	04:00-09:00 and 10:00-18:00 daily	04:00-09:00 and 10:00-18:00 daily	ug C/m <sup>3</sup>	Jan 16 <sup>th</sup> – Feb 15 <sup>th</sup>
PM <sub>10</sub> and PM <sub>2.5</sub> elemental	Streaker sampler (PIXE) – ion beam analysis	1 hr	1 hr	ng/m <sup>3</sup>	Jan 21 <sup>st</sup> – Feb 15 <sup>th</sup>

composition					
PM <sub>2.5</sub> mass concentration	Laser scattering (Met One eSampler)	5 min	1 hr	ug/m <sup>3</sup>	Jan 24 <sup>th</sup> – Feb 15 <sup>th</sup>
NO, NO <sub>2</sub>	Chemiluminescence, blue light converter	1 min	1 hr	ppb	Feb 1 <sup>st</sup> – Feb 15 <sup>th</sup>
carbonyls and ketones	2,4-DNPH cartridges/high performance liquid chromatography	04:00-09:00, 10:00-18:00 and 18:00 -04:00 daily	04:00-09:00, 10:00-18:00 and 18:00 - 04:00 daily	ppb	Feb 4 <sup>th</sup> – Feb 15 <sup>th</sup>

## 5. Meteorology during the MUMBA Campaign

The summer of 2012 - 2013 was the hottest summer on record for Australia at the time [White and Fox-Hughes, 2013]. There were two extremely hot days in the Wollongong region during MUMBA, with maximum temperatures of 40.4 °C on January 8<sup>th</sup> and 42.4°C on January 18<sup>th</sup> 2013 recorded at Bellambi AWS (both below the record of 43.7°C set on January 1<sup>st</sup>, 2006). The campaign encompassed the wettest January day on record for the region, with 139 mm of rain falling at Bellambi AWS between 08:00 on January 28<sup>th</sup> and 08:00 on January 29<sup>th</sup> 2013 (see the top panel of Figure 2).

The lower panel of Figure 2 shows the mean hourly temperature recorded from the 10 m mast at the MUMBA site over the campaign. The two extremely hot days can be clearly seen in this figure. The mean daily maximum temperatures during January 2013 was 25.7°C, which is 0.9°C above the long-term average of 24.8°C and in the 95<sup>th</sup> percentile of monthly mean maximum temperatures for January at Bellambi AWS (using data from 1988 to the present day).

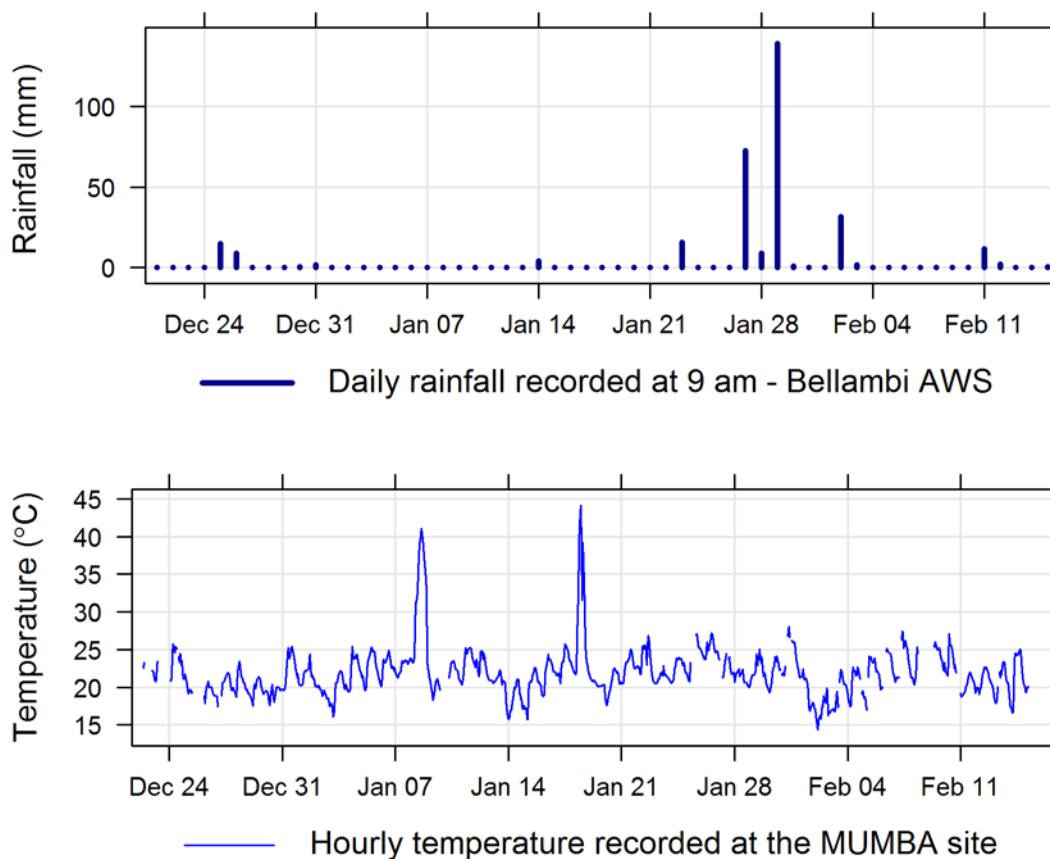


**Figure 2: Upper panel shows a bar chart of daily rainfall in millimeters from Bellambi AWS. Lower panel shows the time-series of mean hourly temperature measured during MUMBA.**

The average wind speed recorded at the MUMBA site during the campaign was 2.8 ms<sup>-1</sup>, and the maximum hourly-averaged wind speed recorded was 9.2 ms<sup>-1</sup>. The 1<sup>st</sup>, 2<sup>nd</sup> (median) and 3<sup>rd</sup> quartiles of the wind speed were 1.4 ms<sup>-1</sup>, 2.6 ms<sup>-1</sup> and 3.9 ms<sup>-1</sup> respectively. Figure 3

shows the composite diurnal cycles of wind speed and wind direction as measured at the main MUMBA site. The general pattern was of a relatively strong sea breeze during the day (~easterly winds of  $3\text{--}4\text{ ms}^{-1}$ ) and of calmer conditions overnight. Westerly winds were more frequent during night time (although north-easterly winds sometimes persisted into the night). This pattern was repeated all over the local region (as shown in data from OEH air quality sites and from the University of Wollongong) [Guérette, 2016].

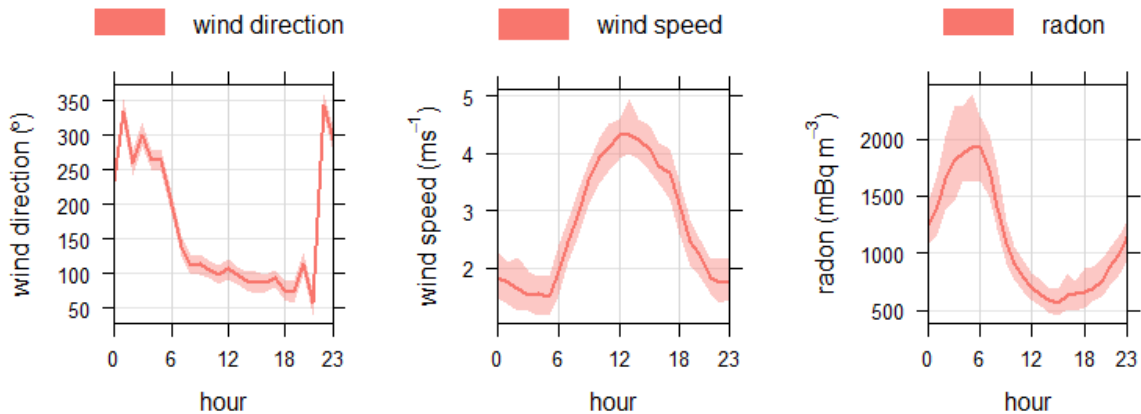


**Figure 3: Observed diurnal cycles of wind direction and wind speed at the main MUMBA site and radon concentration at Warrawong observed during the campaign. (Shaded area shows 95% confidence interval from a bootstrap resampling of the data. See [Carslaw and Ropkins, 2012] for description of this and of calculations of average wind direction).**

The third panel in Figure 3 shows the composite diurnal cycle of radon measured at the ANSTO site in Warrawong. The radon plot shows a build up at night with a peak in the early hours of the morning, indicating a shallower and more stable boundary layer at night than during the day, with the boundary layer at its shallowest around 05:00 or 06:00 AEST. During the day, due to heating at the surface and other processes, the boundary layer grows deeper and more turbulent; this is reflected in the lower radon values observed during the day. Minimum radon levels in the afternoon are also influenced by the fetch of the air reaching the site, with air that has travelled over the ocean containing less radon than air that has travelled over land [Chambers *et al.*, 2015]. In the Wollongong region, an increased boundary layer height and strong sea breezes combine to produce the low radon levels observed in the afternoon.

Comparisons of the winds measured at the MUMBA site during the campaign, to simultaneous measurements at the three air quality sites operated by the Office of Environment and Heritage in the area (at Wollongong, Kembla Grange, and Albion Park), indicated that the wind patterns observed at the MUMBA site were generally representative of the region as a whole [Guérette, 2016]. Long-term average wind data at 15:00 each day are publically available from the Bellambi AWS from 1997 – 2010, and this was used for comparison with the wind data recorded at this time throughout January during the campaign. The MUMBA site in January 2013 was characterised by slightly less frequent northerly

winds and slightly more frequent westerly winds than expected from the long-term average at Bellambi, but otherwise wind patterns were very similar in the two records. The MUMBA site experienced lower wind speeds than the long-term averages at Bellambi (but this may be due to location differences rather than atypical weather patterns) [Guérette, 2016]. Thus we conclude that the measurements made at the MUMBA site during the campaign should be broadly representative of the region, as well as of the summer season.

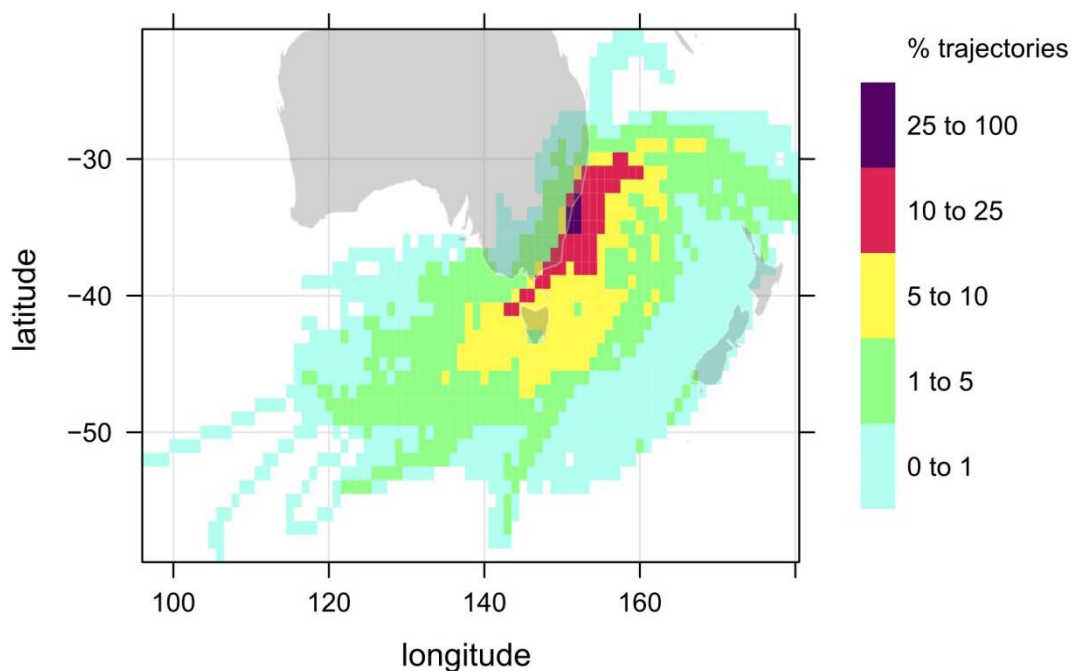


**Figure 4: 96 hour gridded back trajectory frequencies during MUMBA. The surface is coloured by the percentage of total trajectories which pass through each grid-box.**

On a larger scale, the dominant circulation pattern during MUMBA was anti-cyclonic, with the main fetch being principally oceanic (as opposed to continental), which is typical of summer [Chambers *et al.*, 2011]. This is illustrated in Figure 4, which shows a gridded back trajectory frequency plot for 96-hour pre-calculated back trajectories made available for Wollongong through the Openair package [Carslaw and Ropkins, 2012]. The trajectories were calculated using the HYSPLIT trajectory model (Hybrid Single Particle Lagrangian Integrated Trajectory Model; <http://ready.arl.noaa.gov/HYSPLIT.php>) every three hours, from an initial height of 10 metres and propagated backwards in time for 96 hours using the Global NOAA-NCEP/NCAR reanalysis meteorological fields at 2.5° horizontal resolution. The surface of the plot is coloured by the percentage of total trajectories which pass through each grid-box.

## **6. Urban, Marine and Biogenic Influences during the MUMBA Campaign**

The MUMBA campaign was designed to characterise atmospheric composition at the ocean/forest/urban interface and thereby provide a dataset that could be used to test the skill of atmospheric models within a coastal environment. In this section, the major urban, marine and biogenic sources that influence atmospheric composition in the region are described.

The dominant anthropogenic sources in the region are the Port Kembla steelworks, located approximately 10 km south of the main MUMBA site (for PM<sub>2.5</sub>, PM<sub>10</sub>, CO, NO<sub>x</sub> and SO<sub>2</sub>) and motor vehicles (for NO<sub>x</sub>, CO and VOCs) (see: <http://www.npi.gov.au/npidata>). The ocean lies to the east of the site and large forested areas to the west. Outflow from the Sydney basin (80 km to the north) may accompany winds from the north-east.

The impact of the different air-masses sampled can be illustrated using a bivariate polar plot, which shows how a pollutant varies by wind speed and wind direction as suggested by *Carslaw et al* [2006]. Figure 5a shows a bivariate polar plot for CO measured from the main MUMBA site throughout the campaign. Several distinct regions are evident, with the most obvious being the very high amounts of CO that are measured when the site experiences southerly winds with speeds between 2 and 6 ms<sup>-1</sup>. This direction brings air-masses over central Wollongong and also over the industrial area centred on the steelworks at Port Kembla. In contrast, easterly to south-south-easterly winds bring very low amounts of CO to the MUMBA site as the air-masses come from the Pacific Ocean. There were a number of occasions during the campaign when easterly winds brought predominantly marine air to the measurement site. These periods were identified by using radon values below a threshold of 200 mBq m<sup>-3</sup>, indicating minimal terrestrial impact in agreement with back trajectories. One episode in particular, on December 26<sup>th</sup>, 2012, lasted several hours and was characterised by greenhouse gas concentrations similar to those measured in December 2012 at the Cape Grim baseline air pollution station on the north west tip of Tasmania, Australia (40.683°S, 144.689° E) (see <http://www.csiro.au/greenhouse-gases/>). These episodes are explored further in a paper dedicated to the marine air signature during MUMBA [*Guérette et al.*, 2017].

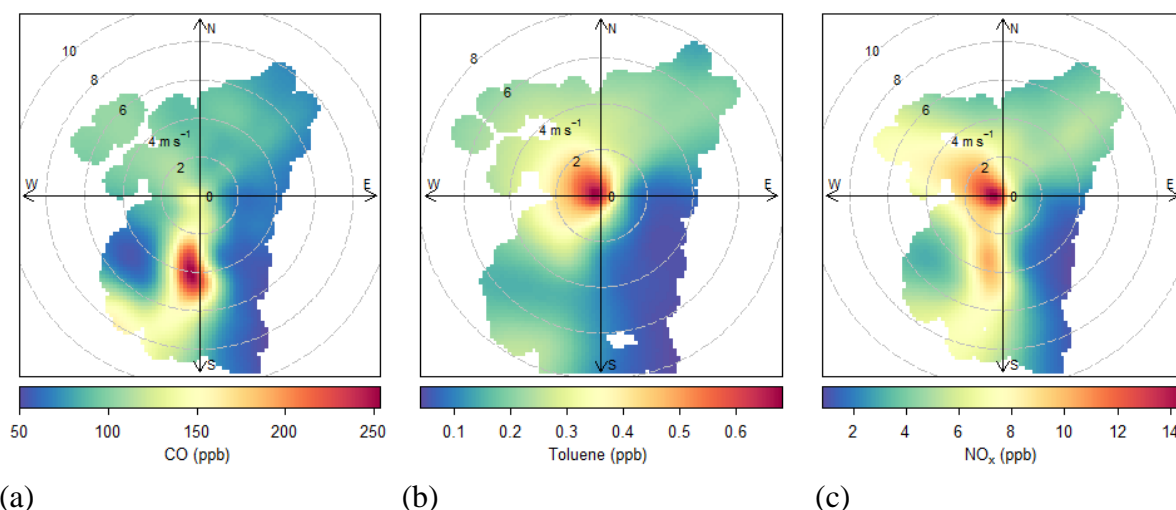


**Figure 5: Bivariate polar plots showing how mole fractions (ppb) of (a) CO, (b) toluene and (c) NO<sub>x</sub> vary as a function of wind speed (ms<sup>-1</sup>) and wind direction at the main MUMBA site during the campaign. Wind speed is represented by the concentric circles and wind direction is shown as compass directions, such that the shape of the coloured area illustrates the wind speeds and directions experienced during the campaign. The colour indicates mean mole fraction measured under the corresponding wind conditions.**

CO mole fractions from the north-east (that also come off the ocean) are nearly double those from the south-south-east, indicating that the MUMBA site may be influenced by outflow from the Sydney basin, 80 km to the north. Elevated CO is also measured from the north-west in the direction of the nearest suburban shopping centre, multilane road and local industrial sites (including a coke-works and mining operations). In contrast, relatively low concentrations are seen from the south-west where there is a steep escarpment and eucalypt forests beyond.

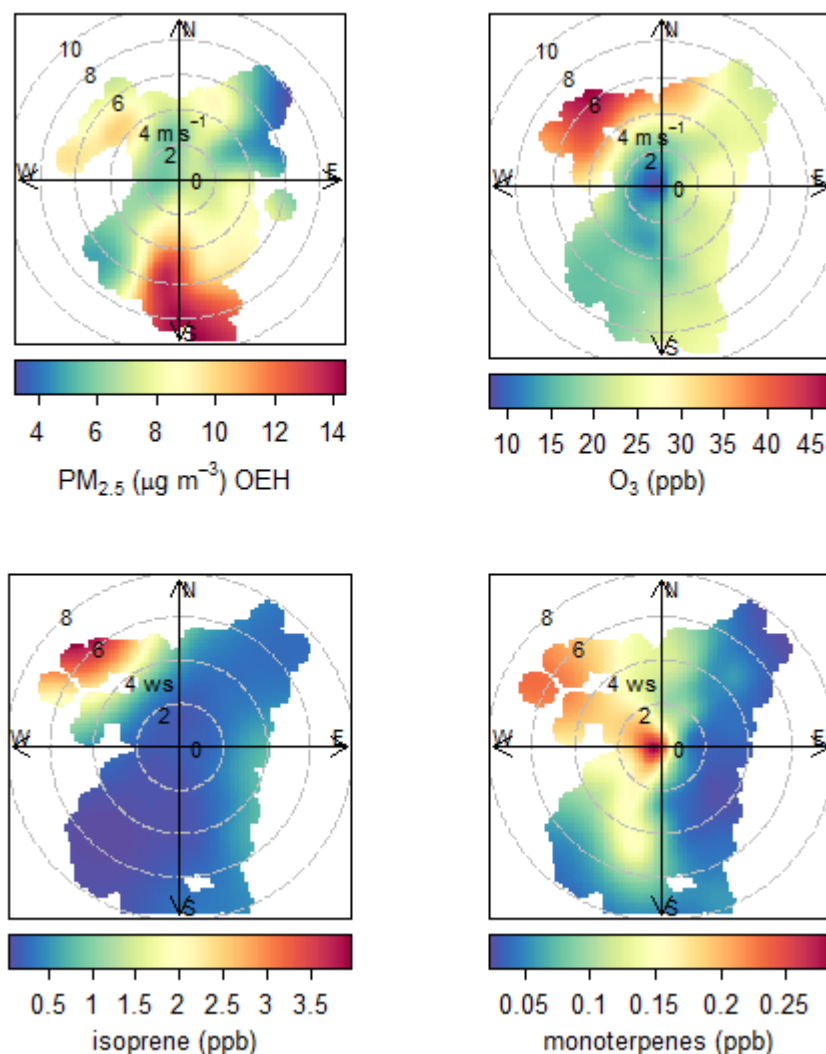
Figure 5b shows the polar bivariate plot for toluene, which is predominantly emitted from motor vehicles and is not emitted from the steelworks. The plot shows the largest concentrations with low wind speeds, as is indicative of local sources building up in the nocturnal boundary layer, however there is a directional bias with much cleaner air to the east. This is due to clean marine air coming from the east and is also obvious in the low amounts of toluene coming from all wind speeds from the south-east. In contrast, there are slightly higher mole fractions of toluene that accompany winds from the north-east, again indicating possible outflow from Sydney or more local pollution to the north that is brought in on the sea breeze.

Figure 5c shows the polar bivariate plot for  $\text{NO}_x$ , which shows a mixture of the features seen in the toluene and CO plots, indicative of a mixture of traffic and industrial sources as expected.

In Figure 6 polar bivariate plots are shown for the main criteria pollutants of concern within the air-shed ( $\text{PM}_{2.5}$  and  $\text{O}_3$ ), along with the most significant biogenic volatile organic compounds, isoprene (PTR-MS  $m/z$  69) and monoterpenes (PTR-MS  $m/z$  137). Both isoprene and monoterpenes show very elevated concentrations with strong north-westerlies, which occurred on the two extremely hot days (January 8<sup>th</sup> and January 18<sup>th</sup> 2013). The monoterpenes are also high with still winds, because (unlike isoprene) these compounds are also emitted during the night and hence build up in the nocturnal boundary layer. Also, under more stable night-time conditions, katabatic flow down the escarpment will bring air predominantly influenced by the eucalypt forests to the site.

The highest  $\text{PM}_{2.5}$  concentrations are seen with strong to moderate winds from the south, which bring industrial sources from the Port Kembla steelworks. Elevated  $\text{PM}_{2.5}$  is also seen with north-westerly winds that bring biogenic influences from the escarpment and densely forested regions beyond. Highest  $\text{O}_3$  concentrations are also seen with the hot north-westerly winds, with the influence of  $\text{NO}_x$  titrating out the  $\text{O}_3$  clearly seen with low concentrations observed at low wind speeds and with wind from the south. The high  $\text{O}_3$  and  $\text{PM}_{2.5}$  values that accompany the high levels of isoprene and monoterpenes, imply that biogenic influences are important for both  $\text{O}_3$  formation and secondary organic aerosol formation in the region. This may be due to having a VOC-limited environment (the formaldehyde to  $\text{NO}_x$  ratio averaged 0.3 over the campaign), coupled to the fact that anthropogenic emissions of VOCs are relatively low in the area, so that biogenic VOCs are extremely important to the overall budget. Despite the importance to air quality, biogenic emissions from Australian eucalypt

forests are poorly understood [Emmerson *et al.*, 2016] and further research is needed to better characterise biogenic emissions in this region of Australia.



**Figure 6:** Bivariate polar plots showing how (a) the concentration of PM<sub>2.5</sub> (μgm<sup>-3</sup>) at the OEH station and mole fractions (ppb) of (b) O<sub>3</sub>, (c) isoprene and (d) monoterpenes at the main MUMBA site, varied as a function of wind speed (ms<sup>-1</sup>) and wind direction during the campaign.

## 7. Summary and Conclusions

The combined datasets from MUMBA provide a useful case study for testing the skill of air quality models in the complex environment of urban, marine and forest influences that exists in coastal Australia, where the majority of its inhabitants live. This overview paper aims to provide the reader with sufficient understanding of the MUMBA campaign to use the datasets as a test case for any air quality model, including an understanding of the Wollongong urban air-shed, regional topography, emissions and meteorology.

During the eight week campaign the MUMBA site experienced some very different conditions, ranging from relatively polluted air (with local urban pollution from traffic and nearby industrial sources), to unpolluted marine air with composition akin to that representative of the remote marine boundary layer measured at the Cape Grim station under baseline conditions. There were two extreme heat events during MUMBA when westerly winds brought strong biogenic influences from nearby forested regions. The measurements of atmospheric composition during these events provide data that could prove to be a valuable test of models of future air quality in a changing climate.

A series of papers are in preparation that describe the main scientific findings from the MUMBA campaign, including articles focusing on: (1) drivers of urban air quality; (2) marine air at 34°S; (3) biogenic emissions of volatile organic compounds; (4) drivers of aerosol loading in the airshed and (5) new particle formation events. In addition, the MUMBA campaign measurements are being used in conjunction with long-term measurements from the OEH air quality network, and campaign data from the Sydney Particle Study campaigns [Keywood *et al.*, 2016a; Keywood *et al.*, 2016b] as observational datasets in a modelling inter-comparison exercise involving four different regional air quality models. The MUMBA data is available from PANGAEA (<https://doi.pangaea.de/10.1594/PANGAEA.871982>) for other researchers wanting to join the inter-comparison exercise or use the data independently to test atmospheric composition simulations in the region.

## **Acknowledgements**

The authors would like to thank all those from the University of Wollongong's Centre for Atmospheric Chemistry and CSIRO's Climate Science Centre group, who helped with the logistics of undertaking an extensive measurement campaign, and in particular Travis Naylor, Graham Kettlewell, Christopher Caldow, Frances Phillips, Jason Ward, James Harnwell and Jenny Fisher. The ANSTO technical staff responsible for installing and maintaining the Warrawong radon detector were Ot Sisoutham and Sylvester Werczynski. Thanks are also due to Kids Uni & the Science Centre for their helpful support, and to David Carslaw (& all the statisticians who developed the relevant 'R' code) for public access to the excellent Openair package for analysis of air quality data. We acknowledge funding from the Australian Research Council (for funding the campaign as part of the Discovery Project DP110101948) and the Clean Air and Urban Landscapes hub of Australia's National Environmental Science Programme (for funding for later analysis of results that was required for producing this manuscript). This research was also supported by Australian Government Research Training Program (RTP) Scholarships.

## References

- Buchholz, R. R., et al. (2016), Source and meteorological influences on air quality (CO, CH<sub>4</sub> & CO<sub>2</sub>) at a Southern Hemisphere urban site, *Atmospheric Environment*, 126, 274-289, doi:<http://dx.doi.org/10.1016/j.atmosenv.2015.11.041>.
- Caine, J. M., et al. (2007), Precursors to Particles (P2P) at Cape Grim 2006: campaign overview, *Environmental Chemistry*, 4(3), 143-150, doi:10.1071/en07041.
- Carshaw, D. C., S. D. Beevers, K. Ropkins, and M. C. Bell (2006), Detecting and quantifying aircraft and other on-airport contributions to ambient nitrogen oxides in the vicinity of a large international airport, *Atmospheric Environment*, 40(28), 5424-5434, doi:10.1016/j.atmosenv.2006.04.062.
- Carshaw, D. C., and K. Ropkins (2012), Openair - An R package for air quality data analysis, *Environmental Modelling and Software*, 27-28, 52-61, doi:10.1016/j.envsoft.2011.09.008.
- Castro, L. M., C. A. Pio, R. M. Harrison, and D. J. T. Smith (1999), Carbonaceous aerosol in urban and rural European atmospheres: estimation of secondary organic carbon concentrations, *Atmospheric Environment*, 33(17), 2771-2781, doi:10.1016/S1352-2310(98)00331-8.
- Chambers, S., A. G. Williams, J. Crawford, and A. D. Griffiths (2015), On the use of radon for quantifying the effects of atmospheric stability on urban emissions, *Atmospheric Chemistry and Physics*, 15(3), 1175-1190, doi:10.5194/acp-15-1175-2015.
- Chambers, S., A. G. Williams, W. Zahorowski, A. Griffiths, and J. Crawford (2011), Separating remote fetch and local mixing influences on vertical radon measurements in the lower atmosphere, *Tellus B*, 63(5), 843-859, doi:10.1111/j.1600-0889.2011.00565.x.
- Cheng, M., I. E. Galbally, S. B. Molloy, P. W. Selleck, M. D. Keywood, S. J. Lawson, J. C. Powell, R. W. Gillett and E. Dunne (2015), Factors controlling volatile organic compounds in dwellings in Melbourne, Australia., *Indoor Air*, doi:10.1111/ina.12201.
- Cheung, H. C., L. Morawska, and Z. D. Ristovski (2011), Observation of new particle formation in subtropical urban environment, *Atmospheric Chemistry and Physics*, 11(8), 3823-3833, doi:10.5194/acp-11-3823-2011.
- Cheung, H. C., L. Morawska, Z. D. Ristovski, and D. Wainwright (2012), Influence of medium range transport of particles from nucleation burst on particle number concentration within the urban airshed, *Atmospheric Chemistry and Physics*, 12(11), 4951-4962, doi:10.5194/acp-12-4951-2012.
- Colomb, A., V. Gros, S. Alvain, R. Sarda-Estève, B. Bonsang, C. Moulin, T. Klupfel, and J. Williams (2009), Variation of atmospheric volatile organic compounds over the Southern Indian Ocean (30-49 degrees S), *Environ. Chem.*, 6(1), 70-82, doi:10.1071/en08072.
- Cope, M. E., et al. (2004), The Australian Air Quality Forecasting System. Part I: Project description and early outcomes, *J. Appl. Meteorol.*, 43(5), 649-662, doi:10.1175/2093.1.
- Cope, M. E., G. D. Hess, S. Lee, K. J. Tory, M. Burgers, P. Dewundege, and M. Johnson (2005), The Australian Air Quality Forecasting System: Exploring first steps towards determining the limits of predictability for short-term ozone forecasting, *Boundary-Layer Meteorology*, 116(2), 363-384, doi:10.1007/s10546-004-2816-2.
- Dunne, E., I. E. Galbally, M. Cheng, P. Selleck, S. B. Molloy, and S. J. Lawson (2017), Comparison of VOC measurements made by PTR-MS, Adsorbent Tube/GC-FID-MS and DNPH-derivatization/HPLC during the Sydney Particle Study, 2012: a contribution

- to the assessment of uncertainty in current atmospheric VOC measurements, *Atmos. Meas. Tech. Discuss.*, 2017, 1-24, doi:10.5194/amt-2016-349.
- Emmerson, K. M., et al. (2016), Current estimates of biogenic emissions from eucalypts uncertain for southeast Australia, *Atmospheric Chemistry and Physics*, 16(11), 6997-7011, doi:10.5194/acp-16-6997-2016.
- Fehsenfeld, F. C., et al. (1990), Intercomparison of NO<sub>2</sub> Measurement Techniques, *J. Geophys. Res.-Atmos.*, 95(D4), 3579-3597, doi:10.1029/JD095iD04p03579.
- Fletcher, C. A., G. R. Johnson, Z. D. Ristovski, and M. Harvey (2007), Hygroscopic and volatile properties of marine aerosol observed at Cape Grim during the P2P campaign, *Environ. Chem.*, 4(3), 162-171, doi:10.1071/en07011.
- Galbally, I. E., S. T. Bentley, and C. P. Meyer (2000), Mid-latitude marine boundary-layer ozone destruction at visible sunrise observed at Cape Grim, Tasmania, 41 degrees 5, *Geophysical Research Letters*, 27(23), 3841-3844, doi:10.1029/1999gl010943.
- Galbally, I. E., S. J. Lawson, I. A. Weeks, S. T. Bentley, R. W. Gillett, M. Meyer, and A. H. Goldstein (2007), Volatile organic compounds in marine air at Cape Grim, Australia, *Environ. Chem.*, 4(3), 178-182, doi:10.1071/en07024.
- Gray, H. A., G. R. Cass, and J. J. Huntzicker (1986), Characteristics of atmospheric organic and elemental carbon particle concentrations in Los Angeles, *Environmental Science and Technology*, 20(6), 580-589.
- Griffith, D. W. T., N. M. Deutscher, C. Caldw, G. Kettlewell, M. Riggenbach, and S. Hammer (2012), A Fourier transform infrared trace gas and isotope analyser for atmospheric applications, *Atmospheric Measurement Techniques*, 5(10), 2481-2498, doi:10.5194/amt-5-2481-2012.
- Guérette, É.-A. (2016), Measurements of VOC sources and ambient concentrations in Australia, PhD Thesis, School of Chemistry, University of Wollongong.
- Guérette, É.-A., et al. (2017), Marine influences during the MUMBA campaign, *Atmospheric Environment (in prep)*.
- Hess, G. D., K. J. Tory, M. E. Cope, S. Lee, K. Puri, P. C. Manins, and M. Young (2004), The Australian Air Quality Forecasting System. Part II: Case study of a Sydney 7-day photochemical smog event, *J. Appl. Meteorol.*, 43(5), 663-679, doi:10.1175/2094.1.
- Hinwood, A. L., et al. (2007), Risk factors for increased BTEX exposure in four Australian cities, *Chemosphere*, 66(3), 533-541, doi:10.1016/j.chemosphere.2006.05.040.
- Husar, R. B., B. Y. H. Liu, and K. T. Whitby (1972), Physical Mechanisms Governing Dynamics of Los-Angeles Smog aerosol, *Journal of Colloid And Interface Science*, 39(1), 211-224, doi:10.1016/0021-9797(72)90155-5.
- Keywood, M., M. Cope, C. P. M. Meyer, Y. Iinuma, and K. Emmerson (2015), When smoke comes to town: The impact of biomass burning smoke on air quality, *Atmospheric Environment*, 121, 13-21, doi:10.1016/j.atmosenv.2015.03.050.
- Keywood, M., et al. (2016a), Sydney Particle Study 1 - Aerosol and gas data collection. v3. , edited by CSIRO, doi:<http://doi.org/10.4225/08/57903B83D6A5D>
- Keywood, M., et al. (2016b), Sydney Particle Study 2 - Aerosol and gas data collection. v1. , edited by CSIRO, doi:<http://doi.org/10.4225/08/5791B5528BD63>
- Lawson, S. J., P. W. Selleck, I. E. Galbally, M. D. Keywood, M. J. Harvey, C. Lerot, D. Helmig, and Z. Ristovski (2015), Seasonal in situ observations of glyoxal and methylglyoxal over the temperate oceans of the Southern Hemisphere, *Atmospheric Chemistry and Physics*, 15(1), 223-240, doi:10.5194/acp-15-223-2015.
- Modini, R. L., Z. D. Ristovski, G. R. Johnson, C. He, N. Surawski, L. Morawska, T. Suni, and M. Kulmala (2009), New particle formation and growth at a remote, sub-tropical coastal location, *Atmospheric Chemistry and Physics*, 9(19), 7607-7621, doi:10.5194/acp-9-7607-2009.

- Monks, P. S., L. J. Carpenter, S. A. Penkett, G. P. Ayers, R. W. Gillett, I. E. Galbally, and C. P. Meyer (1998), Fundamental ozone photochemistry in the remote marine boundary layer: The SOAPEX experiment, measurement and theory, *Atmospheric Environment*, 32(21), 3647-3664, doi:10.1016/s1352-2310(98)00084-3.
- Morille, Y., M. Haeffelin, P. Drobinski, and J. Pelon (2007), STRAT: An automated algorithm to retrieve the vertical structure of the atmosphere from single-channel lidar data, *Journal of Atmospheric and Oceanic Technology*, 24(5), 761-775, doi:10.1175/jtech2008.1.
- Rea, G., C. Paton-Walsh, S. Turquety, M. Cope, and D. Griffith (2016), Impact of the New South Wales fires during October 2013 on regional air quality in eastern Australia, *Atmos. Environ.*, 131, 150-163, doi:10.1016/j.atmosenv.2016.01.034.
- Ristovski, Z. D., T. Suni, M. Kulmala, M. Boy, N. K. Meyer, J. Duplissy, A. Turnipseed, L. Morawska, and U. Baltensperger (2010), The role of sulphates and organic vapours in growth of newly formed particles in a eucalypt forest, *Atmospheric Chemistry and Physics*, 10(6), 2919-2926, doi:10.5194/acp-10-2919-2010.
- Steinbacher, M., C. Zellweger, B. Schwarzenbach, S. Bugmann, B. Buchmann, C. Ordonez, A. S. H. Prevot, and C. Hueglin (2007), Nitrogen oxide measurements at rural sites in Switzerland: Bias of conventional measurement techniques, *J. Geophys. Res.-Atmos.*, 112(D11), D11307, doi:10.1029/2006jd007971.
- Suni, T., et al. (2008), Formation and characteristics of ions and charged aerosol particles in a native Australian Eucalypt forest, *Atmospheric Chemistry and Physics*, 8(1), 129-139, doi:10.5194/acp-8-129-2008.
- Tory, K. J., M. E. Cope, G. D. Hess, S. Lee, K. Puri, P. C. Manins, and N. Wong (2004), The Australian Air Quality Forecasting System. Part III: Case study of a Melbourne 4-day photochemical smog event, *J. Appl. Meteorol.*, 43(5), 680-695, doi:10.1175/2092.1.
- Turpin, B. J., and J. J. Huntzicker (1995), Identification of Secondary Organic Aerosol Episodes and Quantification of Primary and Secondary Organic Aerosol Concentrations During SCAQS, *Atmospheric Environment*, 29(23), 3527-3544, doi:10.1016/1352-2310(94)00276-q.
- Whitby, K. T., R. B. Husar, and B. Y. H. Liu (1972a), The aerosol size distribution of Los Angeles smog, *Journal of Colloid And Interface Science*, 39(1), 177-204.
- Whitby, K. T., B. Y. H. Liu, R. B. Husar, and N. J. Barsic (1972b), The minnesota aerosol-analyzing system used in the Los Angeles smog project, *Journal of Colloid And Interface Science*, 39(1), 136-164.
- White, C. J., and P. Fox-Hughes (2013), Seasonal climate summary southern hemisphere (summer 2012-13): Australia's hottest summer on record and extreme east coast rainfall, *Australian Meteorological and Oceanographic Journal*, 63, 443-456.

## Appendix 1: Details of the Instruments Used

### 1. PTR-MS

An “IONICON” proton transfer reaction mass spectrometer (PTR-MS) from CSIRO operated throughout the MUMBA campaign. The PTR-MS was installed along with the auxiliary equipment that controls the flow rate and incorporates regular sampling of calibration gases and “zero air” [Galbally *et al.*, 2007]. The instrument performed zero measurements twice daily for 40 minutes each time (at 00:50 and at 15:00 local time) by sampling ambient air that had been stripped of volatile organic compounds (VOCs) by passing through a platinum-

coated glass wool catalyst heated to 350°C. A multi-species, single-point calibration was performed daily (from 01:30 until 03:00 local time) by introducing a known flow of calibration standard into the zero air stream. Calibration mole fractions were ~10 to 20 ppb for each VOC present in the standard.

The PTR-MS was operated using  $\text{H}_3\text{O}^+$  ions only and was programmed to scan through its range of mass-to-charge ratios ( $m/z$ ) with a dwell time of one second, for a total cycle time of about three minutes. Mole fractions of volatile organic compounds were calculated from the PTR-MS at the following masses: formaldehyde (mass 31), methanol (mass 33), acetonitrile (mass 42), acetaldehyde (mass 45), acetone (mass 59), isoprene (mass 69); isoprene oxidation products methacrolein and methyl vinyl ketone (mass 71); benzene (mass 79), toluene (mass 93), xylenes (mass 107), trimethyl benzenes (mass 121) and monoterpenes (mass 137). Further details of these measurements, calibrations and corrections can be found in *Guérette* [2016].

## 2. VOC sequencer

From 4<sup>th</sup> to 15<sup>th</sup> February 2013, continuous VOC measurements made using the PTR-MS were supplemented by integrated measurements collected on the VOC sequencer. The VOC sequencer passes air samples through two different adsorbent tubes to collect the VOCs and the carbonyls respectively. These tubes were analysed at CSIRO on a gas chromatography flame ionisation detection/mass spectrometer (GC-FID-MS) for VOCs [*Cheng*, 2015] and HPLC for carbonyls [*Lawson et al.*, 2015], which enables unambiguous species identification (which is not always provided by product ion mass numbers from the PTR-MS) at 5, 8 or 10-hour temporal resolution [*Dunne et al.*, 2017]. Unfortunately, there was a suspected leak on the VOC tube side, (with very low concentrations measured), such that none of these data could be used. In addition there were condensation issues for the carbonyl tubes and only a subset of the species could be determined with confidence. A list of the species measured successfully using the sequencer is given in Table 2.

## 3. Fourier transform Infra-red (FTIR) Trace Gas Analysers

FTIR trace gas analysers measure carbon dioxide ( $\text{CO}_2$ ), methane ( $\text{CH}_4$ ), carbon monoxide ( $\text{CO}$ ) and nitrous oxide ( $\text{N}_2\text{O}$ ) in air with precision and accuracy that meet the World Meteorological Organisation - Global Atmosphere Watch standards for baseline air. In addition the instrument can measure and  $^{13}\text{C}$  in  $\text{CO}_2$  and retains the spectra allowing post analysis for other infrared active trace gases in highly polluted episodes [*Griffith et al.*, 2012]. The instrument ran throughout the whole MUMBA campaign, with the only data interruption due to the cell temperature going above the range calibrated for on the 18<sup>th</sup> January 2013. In theory the instrument could be retrospectively recalibrated at the higher temperatures but since all other instruments had been switched off in the heat this was not attempted. In addition to the instrument at the main MUMBA site, another FTIR trace gas analyser was operated throughout the campaign at the main campus of the University of Wollongong [*Buchholz et al.*, 2016].

#### 4. NO<sub>x</sub> and O<sub>3</sub> Monitors

Throughout the MUMBA campaign O<sub>3</sub> and NO<sub>x</sub> measurements were made using monitors that utilised UV absorption and chemiluminescence techniques respectively. The NO-NO<sub>2</sub>-NO<sub>x</sub> monitor (Thermo Scientific Instruments, model TSI 42i,) detects NO using the chemiluminescence technique. NO<sub>2</sub> is measured via decomposition to NO by passing over a molybdenum converter. The difference between the NO concentrations in the two samples is used to calculate the NO<sub>2</sub> concentration. One issue with this technique is that other nitrates (such as PAN and HNO<sub>3</sub>) may be present and are also converted to NO by molybdenum but with different unknown efficiencies [Steinbacher *et al.*, 2007]. In order to get an indication of the likely level of this problem a second NO<sub>x</sub> monitor from CSIRO was deployed in the last two weeks of the campaign. This NO<sub>x</sub> monitor uses a blue-light converter so that only the NO<sub>2</sub> is converted photolytically to NO [Fehsenfeld *et al.*, 1990]. The analysers were within 5% of each other for both NO and NO<sub>2</sub>.

#### 5. Micro-physical Particle Counters

From 16<sup>th</sup> January to 15<sup>th</sup> February 2013 a suite of microphysical particle counters was operated at the main MUMBA site taking ambient air through an 8 m copper inlet mounted on the mast at a height of ~9.5 m above the surrounding flat area.

An ultrafine condensation particle counter (uCPC, TSI model 3776) measured the total in-situ number concentration of condensation nuclei >3 nm. Particles enter a supersaturated butanol chamber and all particles > 3nm are grown to sizes that were able to be counted with a standard optical counter.

A Cloud Condensation Nuclei Counter (CCNC) made by Droplet Measurement Technologies was used to measure the total number concentration of Cloud Condensation Nuclei (CCN). The instrument operates by similar principle as the CPC, where aerosols are passed through a supersaturated chamber of liquid, except that water is used instead of butanol. Only particles able to act as CCN are thus activated and counted. The instrument was setup to measure particles activated at a supersaturation of 0.5%.

The particle number size distribution from ~14 nm to ~660 nm was measured with a scanning mobility particle sizer (SMPS). The SMPS (TSI model 3080 with DMA 3081 and TSI CPC 3772) ionises particles using radiation from Kr-85 decay. The charged particles then enter an electrostatic column which ramps its voltage to continually select particles based on their charge-mass ratio. Selected particles are then counted by a standard CPC.

Total PM<sub>2.5</sub> aerosol mass concentration measurements were also made using a Met One eSampler utilising laser scattering techniques (from 24<sup>th</sup> January to 15<sup>th</sup> February). The aerosol mass concentration is calibrated via the mass of an integrated sample collected on a filter that was changed weekly.

#### 6. Filter Samplers

Filter samples of total PM<sub>2.5</sub> aerosol were collected twice daily using an Ecotech High Volume Air Sampler (HiVol). Integrated morning samples were collected on filters from

04:00 and 09:00 each day, with integrated afternoon samples from 10:00 to 18:00 each day. Thus two filter changes were required (one between 09:00 and 10:00 and another after 18:00 and before 04:00). The filters were taken back to CSIRO for aerosol chemical composition analysis.

A small section ( $\sim 0.5 \text{ cm}^2$ ) of each filter was punched out and the total collected  $\text{PM}_{2.5}$  aerosol analysed for its total carbon content, elemental carbon (EC) and organic carbon (OC) content using a Thermal Optical Carbon Analyser (Model 2001A). The HiVol instrument logs the total flow of air that has been passed through each filter and so the total carbon, EC and OC in the integrated sample of air can be calculated in  $\mu\text{g}/\text{m}^3$ .

Also deployed was a Streaker Sampler from GNS Science. This sampler slowly rotates a disk holding two filters taking  $\sim 48$  hours for a full revolution. The filters were changed every two days between 09:00 and 10:00. Only a small section of the filter is required for elemental composition analysis such that hourly measurements of black carbon and all elements from sodium to uranium on the periodic table are obtained.

## 7. LIDAR

Throughout the MUMBA campaign ANSTO provided a Leosphere ALS-400 cloud and aerosol LIDAR that measures elastic backscatter at 355 nm, which is proportional to aerosol density. By plotting the (range-corrected) backscatter against height, a vertical profile of aerosol density is created. A negative gradient in aerosol density as represented in the vertical profiles is indicative of a reduction in aerosol density, and therefore a candidate for the boundary layer height. Boundary layer heights were estimated via two methods:

- (1) Visually from plots of the logarithm of the range-corrected 355 nm signal against height
- (2) Using the “STRAT” algorithm [Morille *et al.*, 2007].

Since this technique relies on clear skies and sufficient aerosol loading to provide a strong backscatter signal, it is not always possible to determine the boundary layer height with confidence. Both estimates of boundary layer height with 20-minute resolution are included in the PANGAEA dataset (<https://doi.pangaea.de/10.1594/PANGAEA.871982>).

## 8. Weather Station

Two different weather stations operated during MUMBA providing common meteorological parameters including temperature, humidity, pressure, wind speed and direction. The switch occurred on the 25<sup>th</sup> January when the original (borrowed) weather station was needed for another field campaign. The Digitech system operated at 5-minute resolution and provided wind direction as 16 quadrants only, whereas the original station (Campbell Scientific Inc.) operated at 1-minute resolution and provided wind direction with degree resolution. Both records are available on PANGAEA as hourly averages.

## Appendix 2: List of VOCs Measured

Species	formula	MW	Measurement technique	Time Resolution	n	DL (ppb)	n < DL
formaldehyde	C <sub>2</sub> H <sub>4</sub> O	30.03	DNPH-derivatization/HPLC	04:00 – 09:00	12	0.019	
				10:00 – 18:00	11	0.012	0
				18:00 – 04:00	9	0.009	
			PTR-MS m/z 31	hourly	1027	0.205 0.105 0.186	23
methanol	CH <sub>3</sub> OH	32.04	PTR-MS m/z 33	hourly	1027	0.050 0.033 0.062	0
acetonitrile	C <sub>2</sub> H <sub>3</sub> N	41.05	PTR-MS m/z 42	hourly	1027	0.002 0.001 0.002	0
acetaldehyde	C <sub>2</sub> H <sub>4</sub> O	44.05	DNPH-derivatization/HPLC	04:00 – 09:00	12	0.018	
				10:00 – 18:00	11	0.011	1*
				18:00 – 04:00	9	0.009	
			PTR-MS m/z 45	hourly	1027	0.018 0.007 0.012	0
Glyoxal	C <sub>2</sub> H <sub>2</sub> O <sub>2</sub>	58.04	DNPH-derivatization/HPLC	04:00 – 09:00	12	0.011	
				10:00 – 18:00	11	0.007	0
				18:00 – 04:00	9	0.006	
acetone			PTR-MS m/z 59	hourly	1027	0.010 0.013 0.007	0
Propanal	C <sub>3</sub> H <sub>6</sub> O	58.08	DNPH-derivatization/HPLC	04:00 – 09:00	12	0.011	
				10:00 – 18:00	11	0.007	4
				18:00 – 04:00	9	0.006	
isoprene			PTR-MS m/z 69	Hourly	1029	0.003 0.005 0.003	2
sum of methacrolein and methyl vinyl ketone	C <sub>4</sub> H <sub>6</sub> O	70.09	PTR-MS m/z 71	Hourly	1027	0.004 0.005 0.002	0
methylglyoxal	C <sub>3</sub> H <sub>4</sub> O <sub>2</sub>	72.02	DNPH-derivatization/HPLC	04:00 – 09:00	12	0.006	
				10:00 – 18:00	11	0.003	0
				18:00 – 04:00	9	0.003	
benzene			PTR-MS m/z 79**	hourly	1029	0.010 0.012 0.007	14

toluene			PTR-MS m/z 93		1029	0.005 0.008 0.004	1
hexanal	C <sub>6</sub> H <sub>12</sub> O	100.16	DNPH-derivatization/HPLC	04:00 – 09:00	12	0.008 ppb	
				10:00 – 18:00	11	0.005 ppb	2
				18:00 – 04:00	9	0.004 ppb	
benzaldehyde	C <sub>7</sub> H <sub>6</sub> O	106.12	DNPH-derivatization/HPLC	04:00 – 09:00	12	0.003	
				10:00 – 18:00	11	0.002	1
				18:00 – 04:00	9	0.002	
sum of C <sub>8</sub> H <sub>10</sub> compounds	C <sub>8</sub> H <sub>10</sub>	106.16	PTR-MS m/z 107		1029	0.003 0.016 0.009	13
sum of C <sub>9</sub> H <sub>12</sub> compounds	C <sub>9</sub> H <sub>12</sub>	120.20	PTR-MS m/z 121	hourly	1029	0.003 0.013 0.006	2
sum of monoterpenes			PTR-MS m/z 137	hourly	1029	0.007 0.016 0.007	29

#note that the PTRMS was run under three differing instrumental settings (due to an accidental change in dwell time setting). Thus 3 different detection limits are listed. See metadata in PANGAEA for more details.

\*An additional 11 data points were excluded due to analytical problems